Molecular dynamics simulation of liquid H2O, MeOH, EtOH, Si (OMe) 4, and Si (OEt) 4, as a function of temperature and pressure

ARTICLE · JANUARY 2001

CITATIONS
25

READS
42

3 AUTHORS, INCLUDING:

Richard Richard A Catlow
University College London
994 PUBLICATIONS **25,598** CITATIONS
SEE PROFILE

Geoffrey David Price
University College London
268 PUBLICATIONS **7,773** CITATIONS
SEE PROFILE

Molecular Dynamics Simulation of Liquid H_2O, MeOH, EtOH, $Si(OMe)_4$, and $Si(OEt)_4$, as a Function of Temperature and Pressure

J. C. G. Pereira,*[,†,‡,§] C. R. A. Catlow,[‡] and G. D. Price[§]

The Royal Institution of Great Britain, 21 Albemarle Street, London W1X 4BS, United Kingdom, Department of Geological Sciences, University College London, Gower Street, London WC1E 6BT, United Kingdom, and Materials Engineering Department, Instituto Superior Técnico, Avenida Rovisco Pais, 1000 Lisboa, Portugal

Received: May 17, 2000; In Final Form: October 2, 2000

We use molecular dynamics simulations to model pure liquids, including water (and heavy water), the simplest alcohols (MeOH and EtOH), and the simplest silica alkoxides ($Si(OMe)_4$ and $Si(OEt)_4$), at high pressures and temperatures and under ambient conditions. The same methodology is employed throughout to derive potentials for different species, and the same potentials are used for different thermodynamic conditions. The studies were carried out using two different MD codes, DISCOVER and DL_POLY, with slightly different implementations and force fields, to guarantee that the results would not be sensitive to details of the simulations. The results obtained with both codes for density, enthalpy of vaporization, and radial distribution functions compare very well with experiment, whereas the self-diffusion coefficients are slightly too high. The same general methodologies and sets of potentials should therefore be valid in describing complex liquids, such as silica-based sol−gel solutions, containing water, alcohol, and silica alkoxide, without having to redefine the force field on changing the composition or thermodynamic conditions.

1. Introduction

During the last 25 years, the importance and difficulty of studying the liquid state has stimulated a considerable effort to reproduce the atomistic behavior of simple liquids, using molecular dynamics (MD) and Monte Carlo simulations based on system-specific potentials. Liquid water, methanol, and ethanol are among the most widely studied liquid systems so far, because of both their importance and the wide range of experimental data available. Unfortunately, these studies usually are specific for each liquid, and neither the potentials nor the methodology can be transferred to simulate different systems. To simulate complex solutions, we need to develop general methodologies and sets of potentials that work simultaneously for the many different compositions, temperatures, and pressures used in experimental studies.

In this paper, we report molecular dynamics simulations of water (and heavy water), methanol and ethanol, tetramethoxysilane (TMOS = $Si(OCH_3)_4$), and tetraethoxysilane (TEOS = $Si(OCH_2CH_3)_4$) at a range of pressures and temperatures and under ambient conditions. We employed a common methodology to derive the potential parameters and to generate the simulations for all the liquids; the same potentials were used for all thermodynamic conditions. The results obtained for all these systems and conditions are in good agreement with experimental evidence.

Previous Studies. In 1969, in one of the first simulations of molecular liquids, Barker et al.[1] calculated the energy, specific heat, and radial distribution function of liquid water, using a Monte Carlo technique, with an intermolecular pair potential (R) determined by Rowlinson[2] from the properties of ice and steam. Two years later, Rahman et al.[3] used molecular dynamics to study, for the first time, the static structure and kinetic properties of water, including radial distribution functions and self-diffusion coefficients. These authors used the so-called Ben-Naim and Stillinger (BNS) potentials. At the same time, Narten et al.[4] derived the molecular correlation functions in water, from X-ray diffraction at progressively higher temperatures. A revised potential, ST2, was proposed by Stillinger et al.,[5] who compared the molecular structure and thermodynamic properties in water for the three sets of potentials, R, BNS, and ST2. The same authors also provided a comprehensive review of the early stages of the development of the field.[6] All these potentials use a four-charge model for each water molecule, considered as a rigid body, and a cutoff to truncate the long-range interactions. In Watt's model for water, applied by McDonald,[7] the charges are located in the nucleus, and a Morse potential is used to describe the OH hydrogen bond.

More recently, Jorgensen carried out an extensive set of simulations, using Monte Carlo techniques coupled with NVT (constant number of particles, volume and temperature) and NPT (constant number of particles, pressure and temperature) conditions, Metropolis sampling, and a long-range cutoff. Jorgensen's studies embraced water,[8,9] methanol,[10] ethanol,[11] and other organic liquids,[12−14] applying the so-called transferable intermolecular potential functions (TIPS potentials).

In more recent studies, the Ewald summation procedure has replaced the Coulombic cutoff as the preferred method to describe the long-range interactions, although very similar thermodynamic and structural properties have been found for both methods, for cutoffs larger than 6 Å.[15] The molecular dynamics simulations of liquid water published by Stillinger et al.,[16] which used a revised central force model, were among the first simulations carried out in liquids with an Ewald sum. The comparisons between SPC, ST2, TIPS2, and TIP4P potentials, made by Jorgensen et al.,[17] to determine the structure and self-diffusion

*Corresponding author. Present address: Departmento Engenharia de Materiais, Instituto Superior Técnico, 1000 Lisboa, Portugal. E-mail: carlos@pehoe.civil.ist.utl.pt; Tel, 351-21-8418111; Fax, 351-21-8418132-2.

† Instituto Superior Técnico.

‡ The Royal Institution of Great Britain.

§ University College London.

10.1021/jp0018201 CCC: $20.00
Published on Web 02/10/2001

coefficients of water, were also done using an Ewald sum. The SPC potentials, presented and developed since 1981 by Berendsen et al.,[18] are a particularly simple but successful description of liquid water, with point charges on the oxygen and hydrogen positions, as in the models studied in this work.

The optimization of the Ewald sum to minimize the cutoff error is discussed by Fincham et al.[19] and Kolafa et al.[20] An extensive set of measurements to determine the plateau region of the Ewald energy, similar to the ones presented in our work, is presented by Rycerz et al.[21,22] for ionic systems, such as NaCl and Bi_2O_3.

Monte Carlo simulations in the NVT ensemble, using SPC, TIP4P and TIPS2 potentials have been undertaken by Strauch et al.,[23] to calculate the internal energy, dielectric constant and radial distribution functions of water. The SPC model, similar to the models used in this work, gives the best description of the dielectric constant, according to experiment. Monte Carlo simulations of water have more recently been undertaken by Honda et al.,[24] using a new potential, and various thermodynamic properties, including heat capacity and compressibility, have been reported.

Cell-size effects in liquid methanol have been studied by Casulleras et al.[25] No significant changes were observed for the short and intermediate time-translation motions, but the molecular mobility and the dielectric constant were reported to increase noticeably in the long-time regime.

New potentials to reproduce liquid water and ice 1h, using molecular dynamics, have been proposed by Kumagai et al.[26] and Brodholt et al.[27] Extensive MD simulations of the structure and thermodynamic properties of water at high pressures and temperatures have been reported by Brodholt et al.,[27] using TIP4P, SPC/E (modified SPC), Watanabe and Klein (WK), and Belonoshko and Saxena potentials. Both TIP4P and SPC/E seem to reproduce well the experimental data for these thermodynamic conditions, whereas the WK model is accurate only for densities close to 1 gcm^{-3} and the volumes predicted by the Belonoshko and Saxena potentials, for high pressures, are within 0.3 cm^3 mol^{-1} of those predicted with TIP4P.

Present Study. Our ultimate goal is to simulate complex solutions, containing water, alcohols, silica alkoxides and a wide range of silica clusters, obtained by hydrolysis and condensation reactions. We thus need to develop potentials and methodologies that can automatically describe systems with varying chemical composition and thermodynamic conditions. So far, potentials derived for atomistic simulations, such as those described above, have been designed to be highly accurate but system-specific. In this work we derive potentials that fit the most common properties of these liquids for a wide range of conditions. Molecular dynamics studies of sol−gel solutions, using these potentials, will be reported in future articles.

We used two different MD codes, DISCOVER from Molecular Simulations Inc.[28] and DL_POLY from Daresbury Laboratories,[29] with slightly different implementations and force fields, to analyze how these theoretical differences influence the results and also to guarantee that our main conclusions are essentially independent of the code implementation. We first studied H_2O, MeOH, EtOH, and $Si(OMe)_4$, using DISCOVER at: (1) 10 000 bar and 20° C; (2) 1 bar and 20° C; (3) 1 bar and 80° C. We investigated the density, enthalpy of vaporization, radial distribution functions, and self-diffusion coefficients for all the above systems and thermodynamic conditions. Later we studied H_2O, D_2O, MeOH, EtOH, $Si(OMe)_4$ and $Si(OEt)_4$, using DL_POLY, at (1) 10 000 atm and 20° C, (2) 1 atm and T_b (boiling temperature), and (3) 1 atm and 20 °C. We also studied H_2O, MeOH, and EtOH at 20° C and P_v (vapor pressure). We investigated the density, enthalpy of vaporization, radial distribution functions, and mean square displacements for all systems and thermodynamic conditions mentioned.

2. Computational Details

Simulations with DISCOVER 2.9. We built all systems from blocks with 51 molecules each. To ensure a similar number of atoms in all simulations, we prepared systems containing $51 \times 8 = 408$ molecules of water, methanol, or ethanol, or 51 of TMOS, and TEOS, corresponding to 1224, 2448, 3672, 1071, and 1683 atoms, respectively. In all cases we used a cubic cell with periodic boundary conditions (PBC), a minimum-image convention, a group-based method, and a 9 Å cutoff for all long-range interactions (TEOS simulations were unstable, because of energy fluctuations originated by the group-based criteria). The equations of motion were integrated with a Verlet leapfrog algorithm; using a 1 fs (10^{-15} s) time step. The NPT conditions were simulated by a Berendsen algorithm; 1 and 50 fs were used as the temperature and pressure relaxation times. The ab initio 9−6−1 cff91 force field developed by Molecular Simulations Inc.,[28] containing quartic bond-length and bond-angle terms, a three Fourier term for dihedral angles, and cross terms between the various bond terms, was used in all DISCOVER simulations. The parameters derived for zeolites published by Hill et al.[30] (and obtained from Hartree−Fock ab initio calculations) were used in the silicate clusters. The bond lengths and bond angles for the Si−O−C potentials, not included in the cff91 and silica force fields, were obtained from our previous Density Functional ab initio calculations using the DMOL code,[31,32] whereas the force constants were obtained from geometric averages of the Si−O−Si and C−O−C similar interactions. The partial charges for all atoms were obtained by multiplying by 2.6 the Hirshfeld charges calculated with DMOL for each optimized individual molecule. This factor was chosen as the best compromise to reproduce experimental data for all liquids and thermodynamic conditions. The charges thus obtained are similar to other sets proposed by previous models; in particular, the water charges are very close to the charges proposed by the SPC model.

To avoid overlaps between the molecules and to allow them to move freely to equilibrium positions, we initialized all liquid systems, disposing the molecules first along cubic lattice positions inside a cubic cell with low density of ca. 0.25 g/cm^{-3}. Each system was then submitted to NPT Molecular Dynamics, using ambient temperature and very high pressure, usually 10 000 bar, to force the molecules to interact more strongly before finally decreasing the pressure to 1 bar and allowing the system to relax to ambient conditions. The equilibration and sampling times were set to 19.5 and 0.5 ps (500 time steps), respectively. Preliminary tests covering intramolecular energy, force field, cutoff, run time, system size, time step, and CPU time were carried out.

Simulations with DL_POLY 1.1. As before, we used a cubic cell containing 408 molecules of water, heavy water, methanol, or ethanol, or 51 molecules of TMOS and TEOS. Again we employed PBC conditions, a minimum-image convention, a Verlet leapfrog integration algorithm and a Berendsen NPT ensemble. An Ewald sum with $\alpha = 0.30$ and $q_{max} = 6$ was used to calculate the long-range Coulombic interactions for all systems and thermodynamic conditions. Contributions for energy and pressure due to the van der Waals interactions that are longer than the real-space cutoff were estimated using long-range corrections, as described by Allen and Tildesley.[33] Improvements over the previous DISCOVER simulations

TABLE 1: Calculated and Experimental Density of Water, Methanol, Ethanol, TMOS, TEOS, and Heavy Water for Several Conditions of Pressure and Temperature, Obtained from Atom-Based (DL_POLY) Simulations with an Ewald Sum after 24.0 ps of Equilibration and 1.0 ps of Collecting Time[a]

	Density/g cm^{-3} Calculated (Experimental)					
	H_2O	MeOH	EtOH	$Si(OMe)_4$	$Si(OEt)_4$	D_2O
20.0 °C	1.215	1.007	1.006	1.277	1.191	
10 000 atm	(1.245)[34]	(1.052)[34]	(1.050)[34]			
20.0 °C	1.020	0.773	0.773	1.040	0.941	1.145
1.0 atm	(0.998)[34,35]	(0.791)[34]	(0.789)[34]	(1.02)[36]	(0.93)[36]	(1.105)[38]
T_b	0.947	0.733	0.705	0.933	0.788	
1.0 atm	(0.958)[34]	(0.753)[34]	(0.735)[34]			
T_b[36]/°C	100.0	64.5	78.3	121	169	

[a] Experimental values are from refs 34−36 and 38.

included an atom-based method to calculate interactions, a larger cutoff of 11.0 Å for the real-space contributions (although a cutoff of 10.5 Å was used in water and TMOS because the cell box was not big enough to support a 11.0 Å cutoff under the minimum image convention), and a smaller time step of 0.5 fs. As before, the initial configurations were prepared with a low density, to avoid overlaps and make the equilibration easier; they were then compressed to 10 000 atm, relaxed to ambient conditions, and finally heated to the boiling point. The equilibration and sampling times were set to 24.0 and 1.0 ps (2.000 time steps), respectively. To investigate how the simulation time affects the results, particularly the self-diffusion coefficients, we simulated water, methanol, and ethanol at 1 atm and 20 °C for 50 ps (100 000 time steps).

As before, the 9−6−1 cff91 force field developed by Molecular Simulations Inc.,[28] the silica potentials,[30] and the Si−O−C parameters were used in all DL_POLY simulations, but the cross terms were not applied. Not only is the influence of these terms small and their accuracy questionable, but they make calculations slower and more complex. However, the terms might be important in calculations of vibrational properties, which are not considered in this work. To fit the experimental data, we obtained the atomic Coulombic charges by multiplying by 2.7 (instead of 2.6 as before) the Hirshfeld atomic charges of each molecule optimized in our earlier density functional theory (DFT) studies. The full set of partial charges used with DL_POLY, calculated in exactly the same way for all liquids studied, is presented in Appendix A. The sets of potentials used for oxygen, hydrogen, carbon, and silicon, the same for all thermodynamic conditions, are analyzed in Appendix B. A detailed analysis of the Ewald sum parameters used with DL_POLY, which are exactly the same for all liquids studied, is presented in Appendix C.

Intramolecular nonbond energies depend on the scaling factors, which we made equal to 0.0 for 1−3 interactions and 1.0 for 1−4 interactions (the usual values), in both DL_POLY and DISCOVER. (Thus, for example, the Coulombic energy for methanol is positive, because only repulsions between methyl and hydroxyl hydrogens are taken into account.) Both DISCOVER and DL_POLY simulations were implemented using a fully atomistic force field, obtained entirely from ab initio calculations. Technical details and further references about all the methods mentioned here can be found elsewhere.[33]

3. Results

We now report the results obtained for density, enthalpy of vaporization, radial distribution functions, and self-diffusion coefficients for all the liquids we studied. For the sake of brevity, we will focus on the results obtained with DL_POLY, comparing them with the results obtained with DISCOVER whenever relevant.

TABLE 2: Calculated and Experimental Densities of Water, Methanol, Ethanol, and TMOS for Several Conditions of Pressure and Temperature Obtained from Group-Based (DISCOVER) Simulations with a Coulombic Cutoff after 19.5 ps of Equilibration and 0.5 ps of Collecting Time[a]

	Density/g cm^{-3} Calculated (Experimental)			
	H_2O	MeOH	EtOH	$Si(OMe)_4$
20.0 °C	1.204	0.996	0.984	1.229
10 000 bar	(1.246)[34]	(1.052)[34]	(1.050)[34]	
20.0 °C	1.009	0.747	0.730	1.042
1.0 bar	(0.998)[34,35]	(0.791)[34]	(0.789)[34]	(1.02)[36]
80.0 °C	0.946	0.694	0.649	1.013
1.0 bar	(0.972)[34]	(0.736)[34]	(0.737)[34]	

[a] Experimental values are from refs 34, 35, and 36.

Density. The NPT ensemble is becoming increasingly important in molecular simulation studies, and several methods have been developed for such simulations. Density was chosen as one of the test properties in this work, because of its importance and the extensive range of experimental data available, as a function of temperature and pressure. Density is easy to calculate in a periodic boundary system and simultaneously provides a good test of the intermolecular forces, the cutoff criterion and the NPT method used.

The densities of water, heavy water, methanol, ethanol, and TMOS and TEOS calculated with DL_POLY for the various conditions of pressure and temperature studied in this work are reported in Table 1, together with the experimental results. The densities of water, methanol, ethanol, and TMOS calculated with DISCOVER are reported in Table 2.

In general, the agreement between calculated and experimental values is very good for all systems and thermodynamic conditions, and improves noticeably when DISCOVER is replaced by DL_POLY, which uses a more sophisticated MD method. Simulations of liquid TEOS, which were too unstable, due to the group-based criteria implemented by DISCOVER (used to determine which is the nearest molecular image and whether that molecule is inside the cutoff region), are undertaken for the first time with DL_POLY, using the atom-based criteria. The densities of methanol and ethanol are closer to the experimental values when calculated with DL_POLY. In general, the densities at high pressure (10 000 atm) and high temperature (T_b) increase with DL_POLY and are noticeably closer to the experimental values. The largest difference between calculated and experimental values (MetOH at 10 000 atm) is now 0.045 g/cm^3, corresponding to a relative error of only 4.2%.

These are significant results, considering that exactly the same methodology was used in all cases. The same potentials are used at ambient conditions, high pressure, and high temperature. The charges were obtained by multiplying the ab initio charges always by the same factor, in a completely general procedure. Hirshfeld charges were used because they are implemented in

TABLE 3: Energy Contributions (Bond, Angle, Dihedral, Coulombic, van der Waals, Potential, Kinetic) Obtained from DL_POLY Simulations of 408 Molecules of Water and Heavy Water, in Condensed Phase (Pt, pt, and pT) and in Gas Phase (Vt and VT), for a Pressure $P = 10\,000$ atm or $p = 1$ atm and a Temperature $t = 20$ °C or $T = 100$ °C, with a Collection Time of 2000 Time steps (1 ps)

Energy/kcal mol^{-1}						
	H_2O				D_2O	
	Pt	pt	pT	Vt	VT	pt
bond	207.7	252.8	327.7	83.5	105.4	262.4
angle	250.6	224.3	247.0	97.7	109.1	239.2
dihed	0.0	0.0	0.0	0.0	0.0	0.0
Coul.	−4389.2	−4067.4	−3722.9	0.0	0.0	−4117.6
vdW	149.4	−32.2	−56.6	0.0	0.0	−23.9
poten	−3781.6	−3622.5	−3204.8	181.2	214.5	−3640.0
kinet	1068.7	1068.7	1360.3	1068.7	1360.3	1068.7
totals	−2712.9	−2553.9	−1844.5	1249.9	1574.8	−2571.3

TABLE 4: Energy Contributions (Bond, Angle, Dihedral, Coulombic, van der Waals, Potential, Kinetic) Obtained from DL_POLY Simulations of 408 Molecules of Methanol, in Condensed Phase (Pt, pt, and pT) and in Gas Phase (Vt and VT), for a Pressure $P = 10\,000$ atm or $p = 1$ atm and a Temperature $t = 20$ °C or $T = 64.5$ °C, with a Collection Time of 2000 Timesteps (1 ps)

Energy/kcal mol^{-1}					
	MeOH				
	Pt	pt	pT	Vt	VT
bond	574.8	607.3	721.8	424.7	491.6
angle	809.5	805.2	914.5	665.5	739.7
dihed	−678.4	−681.9	−670.4	−551.7	−554.8
Coul.	5253.3	5525.6	5747.6	8123.2	8122.6
vdW	−816.0	−852.5	−824.7	0.4	0.4
poten	5143.3	5403.7	5888.8	8662.0	8799.5
kinet	2138.2	2138.2	2462.9	2138.2	2462.8
totals	7281.5	7541.9	8351.6	10800.2	11262.3

the DMOL code, but similar results should be obtained using other ab initio charges, provided they present the right chemical trends. A single set of potentials was used for carbon and silicon, although three and four different environments were considered for hydrogen and oxygen, respectively. These too could probably be reduced to a single environment without compromising the quality of the results.

In fact, when a Molecular Mechanics force field, which is essentially composed of intramolecular, van der Waals and Coulombic intermolecular interactions, is used, the density of a liquid is likely to be essentially determined by the short- and medium-range Coulombic interactions and the very short-range van der Waals repulsions. A comparatively smaller contribution comes from the bonding interactions, which become important only at high pressure (because of compactation effects) and at high temperature (because of vibrational effects).

Energy. We analyzed separately the intramolecular and intermolecular Coulombic and van der Waals interactions for all liquids and thermodynamic conditions by comparing the partial energies in condensed- and gas-phase conditions, as reported in Tables 3−7. As expected, the intermolecular energy ($E_{gas} - E_{liq}$) increases with pressure and decreases with temperature, for all systems, with both DL_POLY and DISCOVER. We note that with DISCOVER, ($E_{gas} - E_{liq}$) was obtained by comparing the liquid energy per molecule with the energy of a single molecule (rotational and translational degrees of freedom are not discarded by DISCOVER) averaged over a large interval of time (1.5 ns to equilibrate plus 1.0 ns to collect data), whereas with DL_POLY, (E_{gas}) was calculated by

TABLE 5: Energy Contributions Obtained from DL_POLY Simulations of 408 Molecules of Ethanol, in Condensed Phase (Pt, pt, and pT) and in Gas Phase (Vt and VT), for a Pressure $P = 10\,000$ atm or $p = 1$ atm and a Temperature $t = 20$ °C or $T = 78.3$ °C, with a Collection Time of 2000 Timesteps (1 ps)

Energy/kcal mol^{-1}					
	EtOH				
	Pt	pt	pT	Vt	VT
bond	984.9	978.2	1166.7	1161.2	1354.2
angle	1531.1	1523.9	1762.2	1845.0	2076.4
dihed	−2090.9	−2100.2	−2080.0	−2097.2	−2054.4
Coul.	−22862.0	−22439.0	−21996.0	−20341.0	−20298.0
vdW	−587.5	−591.6	−457.8	953.3	966.9
poten	−23024.0	−22628.0	−21604.0	−18479.0	−17954.0
kinet	3207.8	3207.8	3845.7	3207.8	3845.7
totals	−19816.0	−19421.0	−17759.0	−15271.0	−14109.0

TABLE 6: Energy Contributions (Bond, Angle, Dihedral, Coulombic, van der Waals, Potential, Kinetic) Obtained from DL_POLY Simulations of 51 Molecules of TMOS, in Condensed Phase (Pt, pt, and pT) and in Gas Phase (Vt and VT), for a Pressure $P = 10\,000$ atm or $p = 1$ atm and a Temperature $t = 20$ °C or $T = 121$ °C, with a Collection Time of 2000 Timesteps (1 ps)

Energy/kcal mol^{-1}					
	$Si(OMe)_4$				
	Pt	pt	pT	Vt	VT
bond	331.2	346.1	448.7	342.5	463.7
angle	688.9	705.4	824.9	737.0	879.5
dihed	−524.5	−527.3	−508.9	−510.5	−493.4
Coul.	8885.5	8948.3	9009.3	9206.1	9207.3
vdw	−647.9	−632.2	−546.2	−69.9	−62.7
poten	8733.2	8840.4	9227.9	9705.1	9994.4
kinet	935.0	935.0	1257.1	935.0	1257.1
totals	9668.2	9775.4	10485.0	10640.0	11252.0

TABLE 7: Energy Contributions (Bond, Angle, Dihedral, Coulombic, van der Waals, Potential, Kinetic) Obtained from DL_POLY Simulations of 51 Molecules of TEOS, in Condensed Phase (Pt, pt, and pT) and in Gas Phase (Vt and VT), for a Pressure $P = 10\,000$ atm or $p = 1$ atm and a Temperature $t = 20$ °C or $T = 169$ °C, with a Collection Time of 2000 Timesteps (1 ps)

Energy/kcal mol^{-1}					
	$Si(OEt)_4$				
	Pt	pt	pT	Vt	VT
bond	474.7	483.7	714.1	496.0	748.3
angle	924.3	918.5	1252.9	963.5	1330.3
dihed	−1264.2	−1261.1	−1186.5	−1226.2	−1171.9
Coul.	268.3	336.7	382.8	435.1	440.9
vdW	−742.1	−683.8	−498.8	38.6	55.2
poten	−339.1	−205.9	664.5	707.1	1402.8
kinet	1469.8	1469.7	2216.8	1469.7	2216.9
totals	1130.7	1263.8	2881.3	2176.8	3619.7

expanding the liquid cell to a volume large enough to make all intermolecular interactions completely negligible. Calculating (E_{gas}) allows us to analyze separately the intramolecular and intermolecular Coulombic and van der Waals interactions in the corresponding condensed systems. This comparison is only approximate; the intramolecular energies can be noticeably different in these states, because of the distortions resulting from the interactions with the neighbors, as can be seen by inspection of the bond, angle, and dihedral energies.

In general, the intermolecular Coulombic energy contribution in water is larger than in the alcohols and much larger than in the alkoxides. In water at normal conditions, the intermolecular Coulombic contribution accounts for 99.2% of the intermolecu-

lar energy. In the alcohols, methanol and ethanol, this contribution decreases to, respectively, 75.3% and 57.6% of the intermolecular energy. In the alkoxides, TMOS and TEOS, this contribution corresponds only to 31.4 and 12.0% of the total intermolecular energy. This result was expected, because water is much more polar than methanol and ethanol, which in turn are much more polar than TMOS and TEOS, because of TMOS/TEOS almost spherical symmetry. (We note that both TMOS and TEOS are immiscible in water, because of their apolar characteristics, although both are miscible in methanol and ethanol.) The results also predict, correctly, that ethyl-based are less polar than methyl-based molecules, because of the size of the apolar alkyl groups.

As expected, the energy fluctuations and the total energy are slightly lower in heavy water than in water, as the heavier deuterium atoms tend to slow the dynamics in the liquid. However, only the Coulombic energy is lower in heavy water, all other contributions being higher. As the vibrational frequencies decrease, because of the mass increase, the dominant Coulombic forces have more control on the intermolecular interactions and the overall structure of the liquid.

The same behavior is observed to some extent for all systems at high pressure. Although the total energy and the dominant Coulombic energy are systematically lower in these conditions, the bond and van der Waals contributions usually increase. The apolar TMOS and TEOS, where the Coulombic interactions are not dominant, are the only systems in which the van der Waals energy decreases at high pressure. Therefore, in all other systems, at 10 000 atm, the interatomic distances are already smaller than the distance of the minimum of the 9−6 van der Waals potential. In water this happens even at ambient conditions, because the van der Waals energy of water is lower at the boiling point, after the interatomic distances have increased; this is due again to the small influence of the van der Waals interactions in water compared with the Coulombic terms.

In condensed-phase systems, the energy fluctuations essentially increase with the total number of atoms, and consequently only small differences are discernible between the systems discussed here, all of which have a similar number of atoms. However, in gas-phase systems, where each molecule is completely isolated from the others, the energy fluctuations depend instead on the number of atoms in each molecule. Energy fluctuations are consequently very small for water, increasing steadily for methanol, ethanol, TMOS, and TEOS. In the latter system, the gas-phase and condensed-phase fluctuations are almost identical.

Enthalpy of Vaporization. The enthalpy of vaporization is the easiest energy-dependent experimental property with which to compare our results; it is also one of the most important, because it allows us to check directly the intermolecular energy of the system, which is responsible for its state of aggregation. Experimental values for the enthalpy of vaporization usually are obtained either at 1 atm and the boiling temperature or at the equilibrium vapor pressure for lower temperatures. The simplest way to calculate the enthalpy of vaporization from MD simulations is to compare the enthalpy of the gas with the enthalpy of the liquid: $\Delta H_v = H_{gas} - H_{liq} = E_{gas} + PV_{gas} - E_{liq} - PV_{liq}$, where H and E represent molar values, and then neglect PV_{liq} when compared with PV_{gas} and make the perfect gas approximation $PV_{gas} \approx RT$,[9] thus $\Delta H_v \approx E_{gas} - E_{liq} + RT$.

Table 8 compares enthalpies of vaporization calculated from simulations employing DL_POLY and obtained from experiment, for water, methanol, ethanol, TMOS, and TEOS, at the boiling point and 1.0 atm, at 20.0 °C and at the equilibrium vapor pressure, and finally at 20.0 °C and 1.0 atm (although the latter is a nonphysical situation).

TABLE 8: Calculated and Experimental Enthalpy of Vaporization of Water, Methanol, Ethanol, TMOS and TEOS, for Several Conditions of Pressure and Temperature, Obtained from Atom-based (DL_POLY) Simulations with an Ewald Sum

Enthalpy of Vaporization/kcal mol^{-1} Calculated (Experimental)					
	H_2O	MeOH	EtOH	$Si(OMe)_4$	$Si(OEt)_4$
T_b[36]/°C	100.0	64.5	78.3	121	169
T_b	9.12	7.80	9.64	15.82	15.37
1.0 atm	(9.71)[34,37]	(8.41)[34]	(9.21)[34]	(11.5)[39]	(11.0)[39]
P_v[38]/atm	0.023	0.141	0.065		
20.0 °C	9.90	8.51	10.73		
P_v	(10.54)[34,37]	(8.96)[34,37]	(10.02)[34,37]		
20.0 °C	9.91	8.57	10.75	17.54	18.48
1.0 atm					

[a] Experimental values from refs 34 and 36−39.

TABLE 9: Calculated and Experimental Enthalpy of Vaporization of Water, Methanol, and Ethanol for Several Conditions of Pressure and Temperature, Obtained from Group-Based (DISCOVER) Simulations with a Coulombic Cutoff[a]

Enthalpy of Vaporization/kcal mol^{-1} Calculated (Experimental)			
	H_2O	MeOH	EtOH
20 °C/10 000 bar	11.73	10.29	6.47
20 °C/1 bar	11.31	9.60	5.55
80 °C/1 bar	10.92	9.12	4.18
T_b/1 bar	(9.71)[34,37]	(8.41)[34]	(9.21)[34]

[a] Experimental values from refs 34 and 37.

For water, methanol, and ethanol, the agreement between calculated and experimental values is good, both at the boiling point and at 20 °C. The maximum difference, for ethanol at the equilibrium vapor pressure, is 0.71 kcal mol^{-1}, corresponding to a relative error of 7.1%, which is certainly encouraging considering the general approach used in these simulations. The agreement is much less satisfactory, however, for both alkoxides, where the difference between calculated and experimental data amounts to 4.6 and 4.4 kcal mol^{-1}, for TMOS and TEOS, respectively. However, the difference between the two calculated values, 0.45 kcal mol^{-1}, matches almost exactly the difference between the two experimental values of 0.50 kcal mol^{-1}.

The reasons for such large calculated enthalpies of vaporization for TMOS and TEOS can be found by analyzing separately the various components of the intermolecular energy. While in methanol and ethanol, the van der Waals contributions for the internal energy are calculated as 2.1 kcal mol^{-1} and 3.8 kcal mol^{-1}, in TMOS and TEOS the same contributions become 11.0 and 14.16 kcal mol^{-1}, respectively.

Enthalpies of vaporization calculated from simulations employing DISCOVER are shown in Table 9. In general, the results obtained with DISCOVER are less satisfactory than those obtained with DL_POLY. In particular, the enthalpy of vaporization obtained for ethanol, for all conditions of temperature and pressure, is very low compared with experiment. This result probably is related to the existence of different trans and gauche conformations for ethanol and to a strong stabilization of the gauche conformation in the isolated molecule. In fact, for this set of charges, the trans conformation was never obtained when using DISCOVER (either by molecular dynamics or energy minimization techniques), which is probably related to the fact that (as discussed in the Computational Details section)

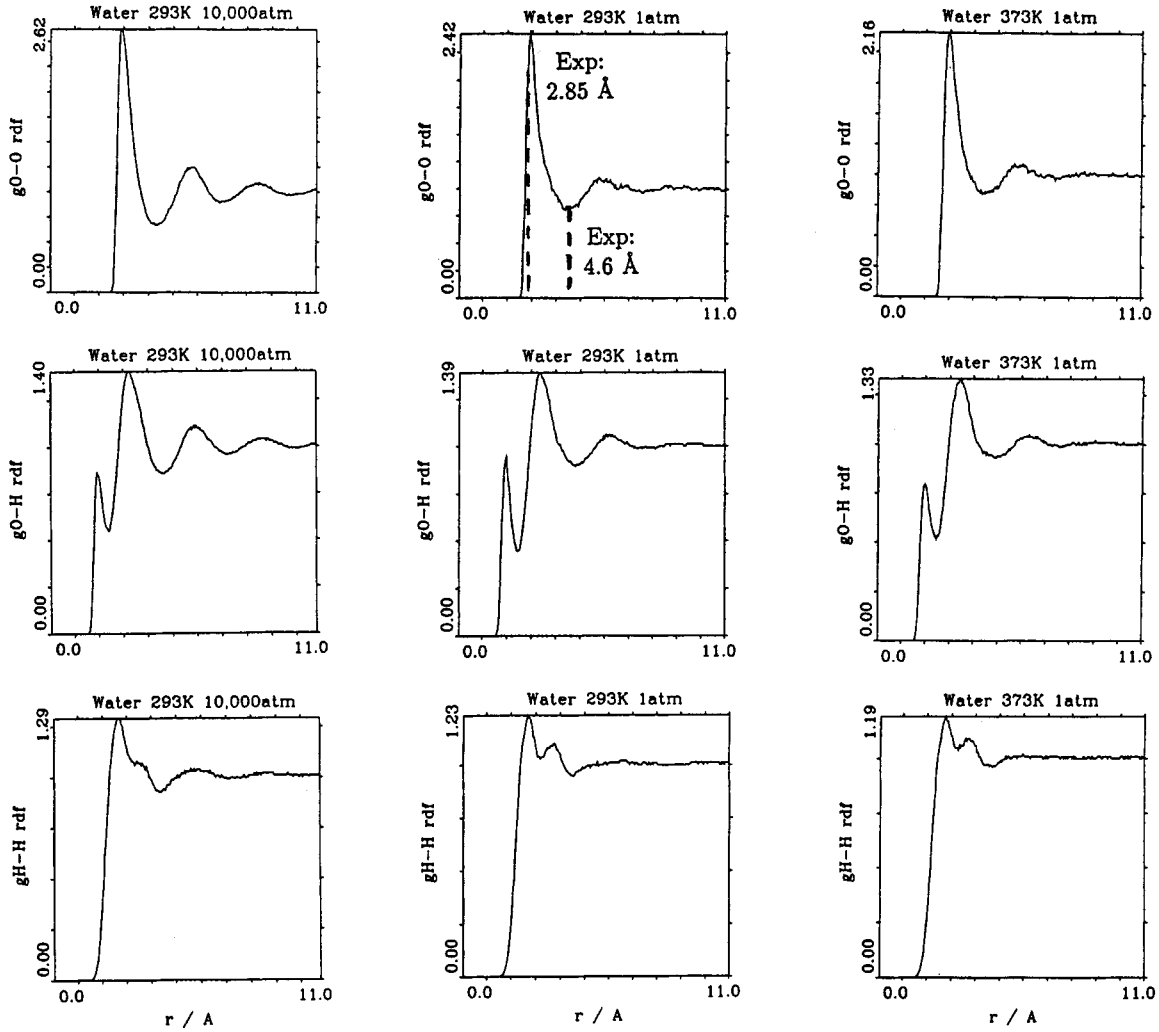

Figure 1. Intermolecular pair distribution functions in water for a pressure of 10 000 or 1 atm and a temperature of 20 or 100 °C, from atom-based (DL_POLY) simulations with an Ewald sum, after 24.0 ps of equilibration time and 1.0 ps of collecting time. X-ray data from ref 9.

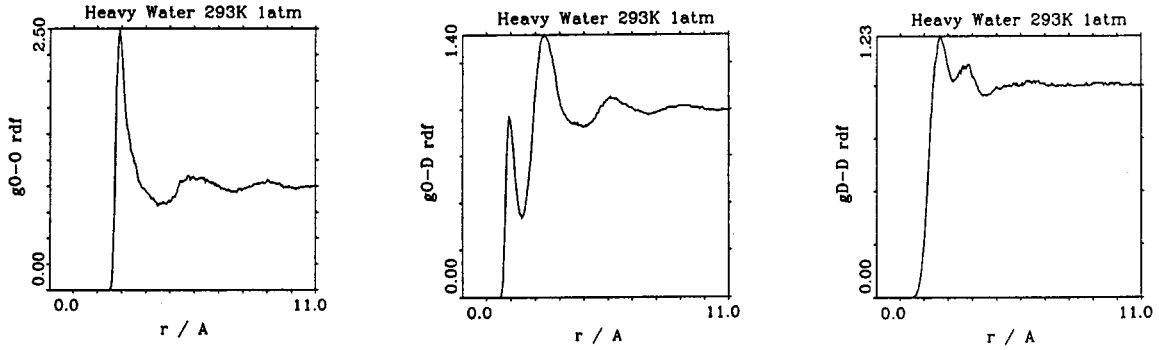

Figure 2. Intermolecular pair distribution functions in heavy water for a pressure of 1 atm and a temperature of 20° C, from atom-based (DL_POLY) simulations with an Ewald sum, after 24.0 ps of equilibration time and 1.0 ps of collecting time.

cross-term bond and angle potentials were used with DISCOVER but not with DL_POLY.

Radial Distribution Function. The intermolecular radial distribution functions are an invaluable tool in studying the liquid structure, and therefore they were calculated in this work for all liquids and thermodynamic conditions studied. Because the total number of pair functions is quite large, we report here only those considered to be more important, just as in Jorgensen's work.[8,10,11] We show only the pair functions calculated with DL_POLY because these simulations are more accurate and the distribution functions are very similar to those obtained with DISCOVER. Radial distribution functions (RDFs) were calculated up to a maximum distance of 11.0 Å, which was the real cutoff used in all methanol, ethanol and TEOS simulations (for water and TMOS, a cutoff of 10.5 Å was used, because of the smaller cell boxes, as described in the Computational Details section).

The three O−O, O−H, H−H interactions in water and heavy water are presented in Figures 1 and 2, respectively. The six O−O, O−H_o, H_o−H_o, C−C, C−O, C−H_o methanol interactions and ten O−O, O−H_o, H_o−H_o, C_2−C_2, C_3−C_3, C_2−C_3, O−C_2, O−C_3, C_2−H_o, C_3−H_o ethanol interactions are shown in Figures 3, 4, and 5. The six Si−Si, Si−O, O−O, C−C, C−O, O−H TMOS interactions and six Si−Si, Si−O, O−O, C_3−C_3, C_3−

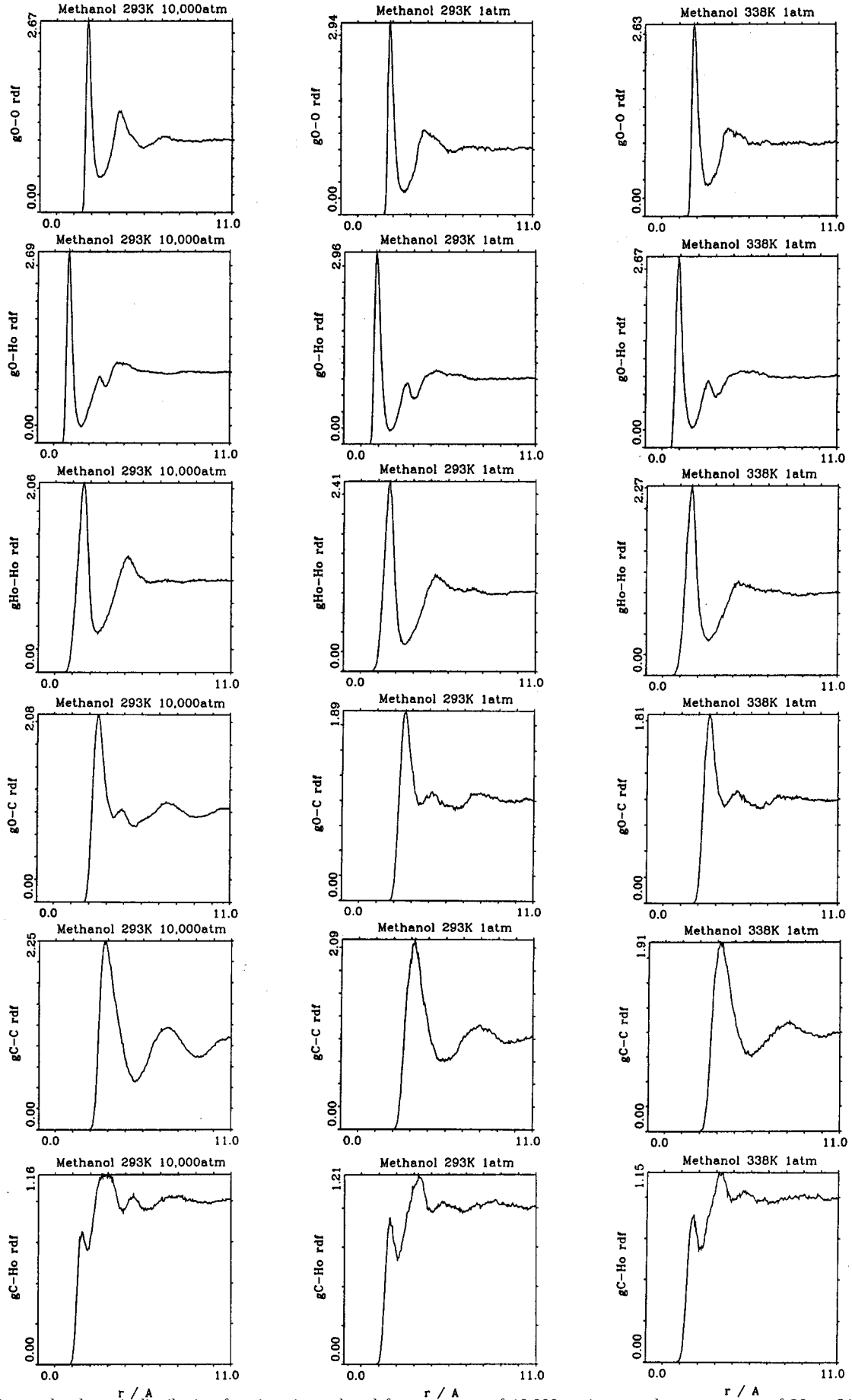

Figure 3. Intermolecular pair-distribution functions in methanol for a pressure of 10 000 or 1 atm and a temperature of 20 or 64.5 °C, from atom-based (DL_POLY) simulations with an Ewald sum, after 24.0 ps of equilibration time and 1.0 ps of collecting time.

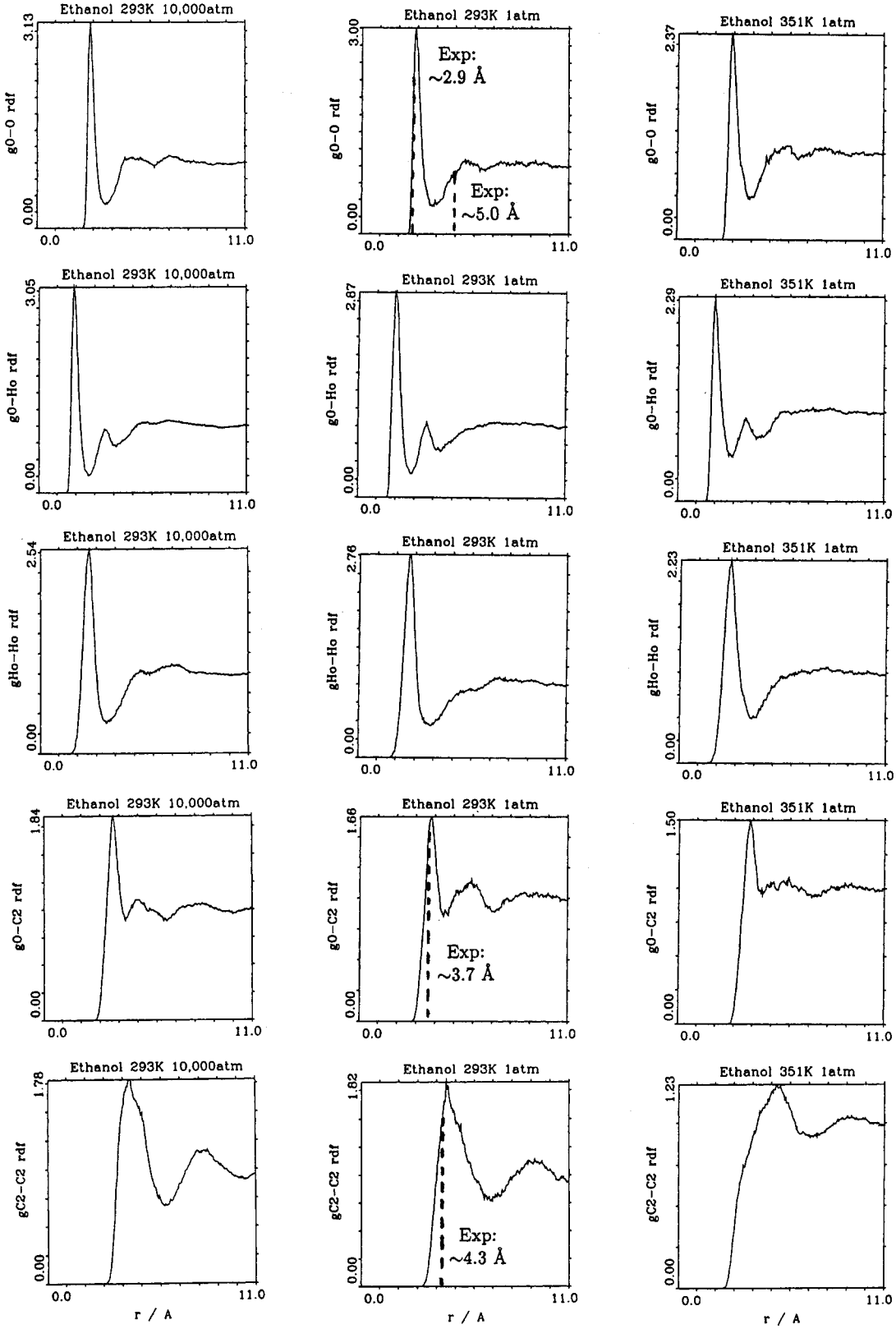

Figure 4. Intermolecular pair-distribution functions in ethanol for a pressure of 10 000 or 1 atm and a temperature of 20 °C or $T = 78.3$ °C, from atom-based (DL_POLY) simulations with an Ewald sum, after 24.0 ps of equilibration time and 1.0 ps of collecting time. X-ray data are from ref 11.

O, O−H_3 TEOS interactions are reported in Figures 6 and 7, respectively.

These results, obtained with DL_POLY (using an Ewald sum, atom-based method, and no cross terms), are very similar to the results calculated with DISCOVER (using a Coulombic cutoff, group-based algorithm, and cross-terms potentials), showing that they can be reproduced using different codes, with different methodologies and even slightly different potentials. The O−O first peak in water is well-positioned, between 2.9 and 3.0 Å, and is lower than with DISCOVER, in better

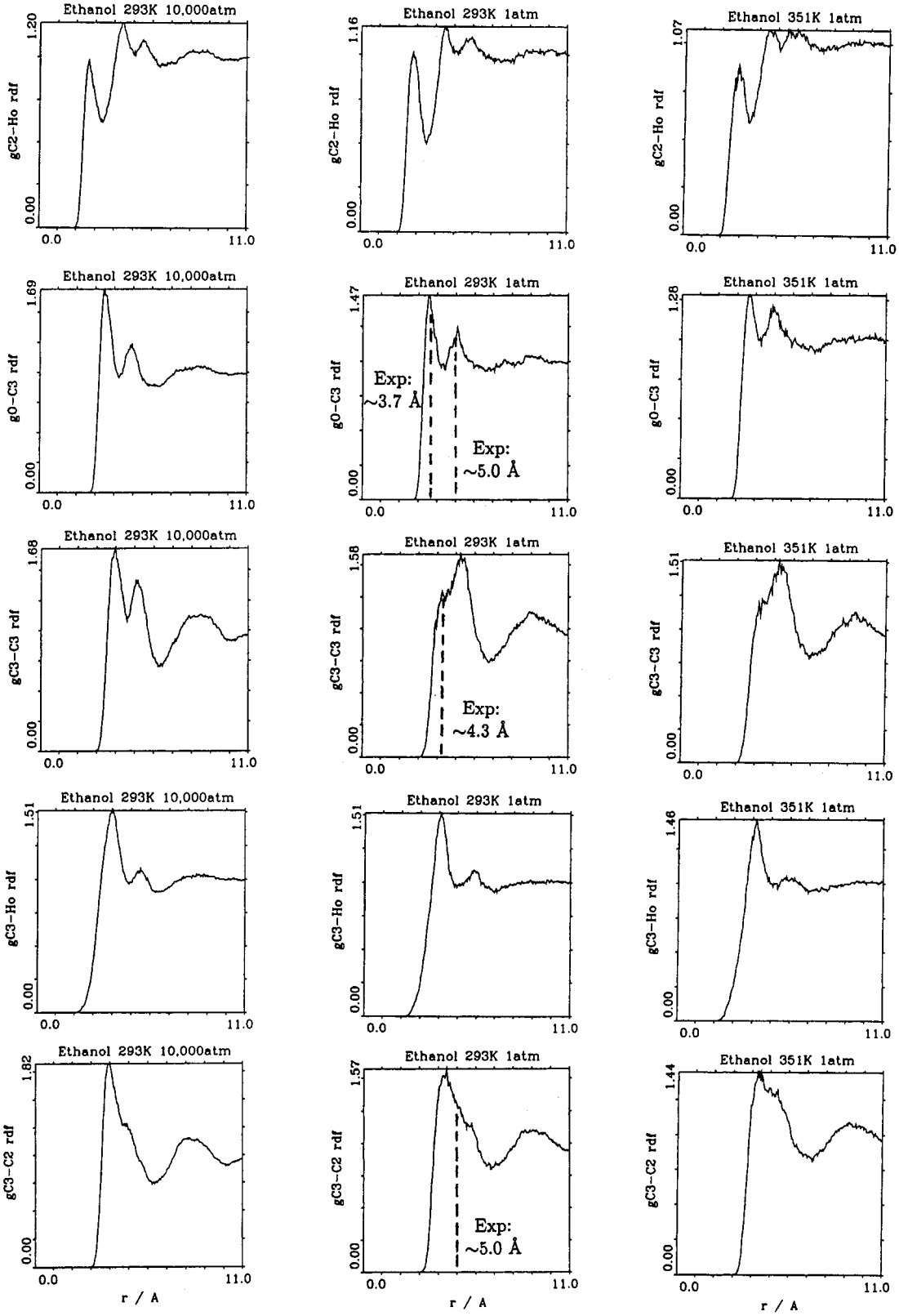

Figure 5. Intermolecular pair-distribution functions in ethanol (cont.) for a pressure of 10 000 or 1 atm and a temperature of 20 °C or $T = 78.3$ °C, from atom-based (DL_POLY) simulations with an Ewald sum, after 24.0 ps of equilibration time and 1.0 ps of collecting time. X-ray data are from ref 11.

agreement with experiment; however, the position of the second peak, at about 5.7 Å, is still too large.[4] At the boiling point the second peak is still visible, whereas at high pressure, a third peak appears at 8.5 Å. In heavy water, the liquid structure is more defined, because of the lower deuterium velocities; the third peak is already visible, but the first two peaks are almost equal, as in water.

In methanol and ethanol, the O−O first peak is higher than in water, but it appears at the same position. In both alcohols, a pronounced valley is seen between 3.5 and 4.5 Å, before the

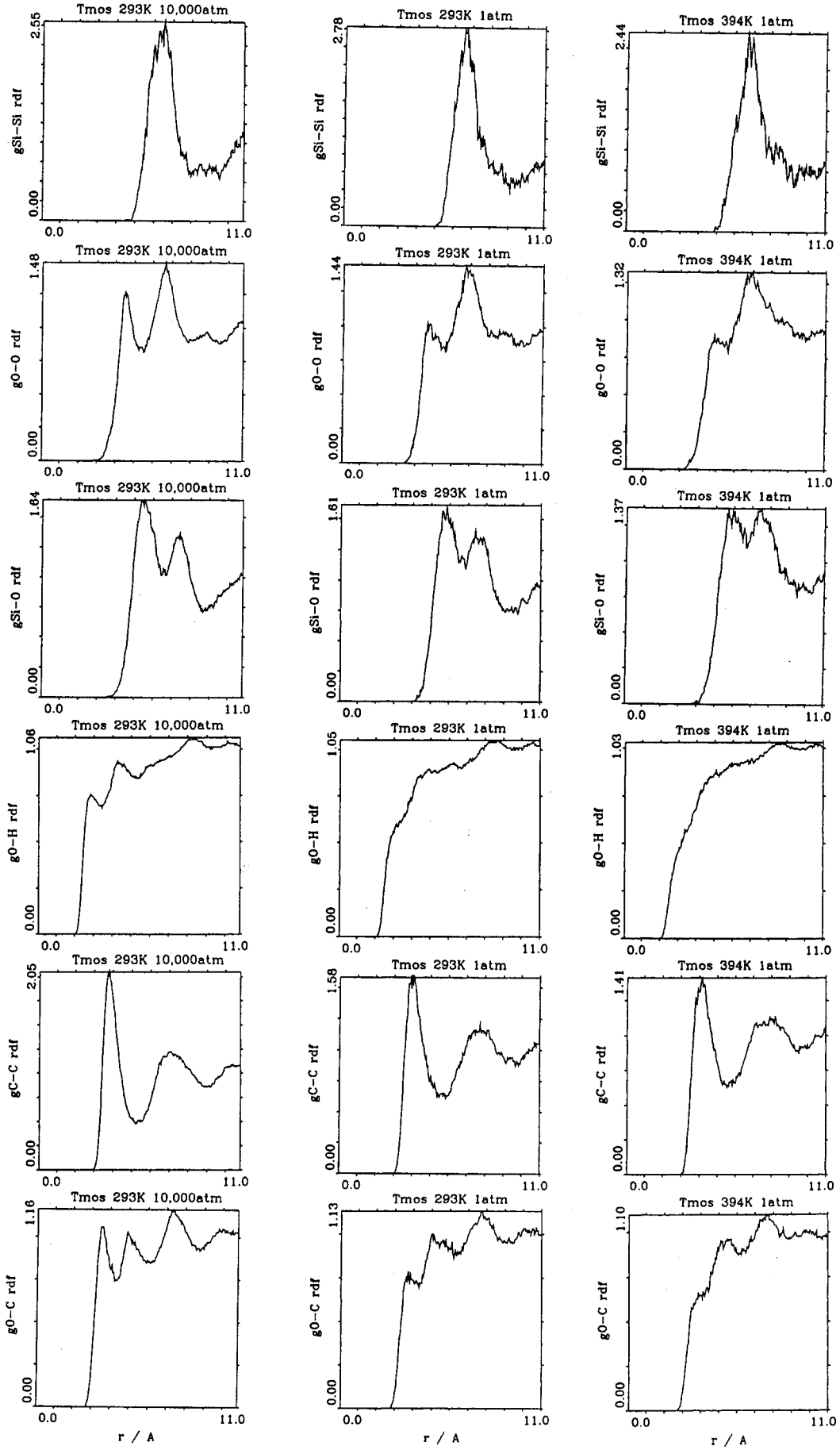

Figure 6. Intermolecular pair-distribution functions in TMOS for a pressure of 10 000 or 1 atm and a temperature of 20 or 121 °C, from atom-based (DL_POLY) simulations with an Ewald sum, after 24.0 ps of equilibration time and 1.0 ps of collecting time.

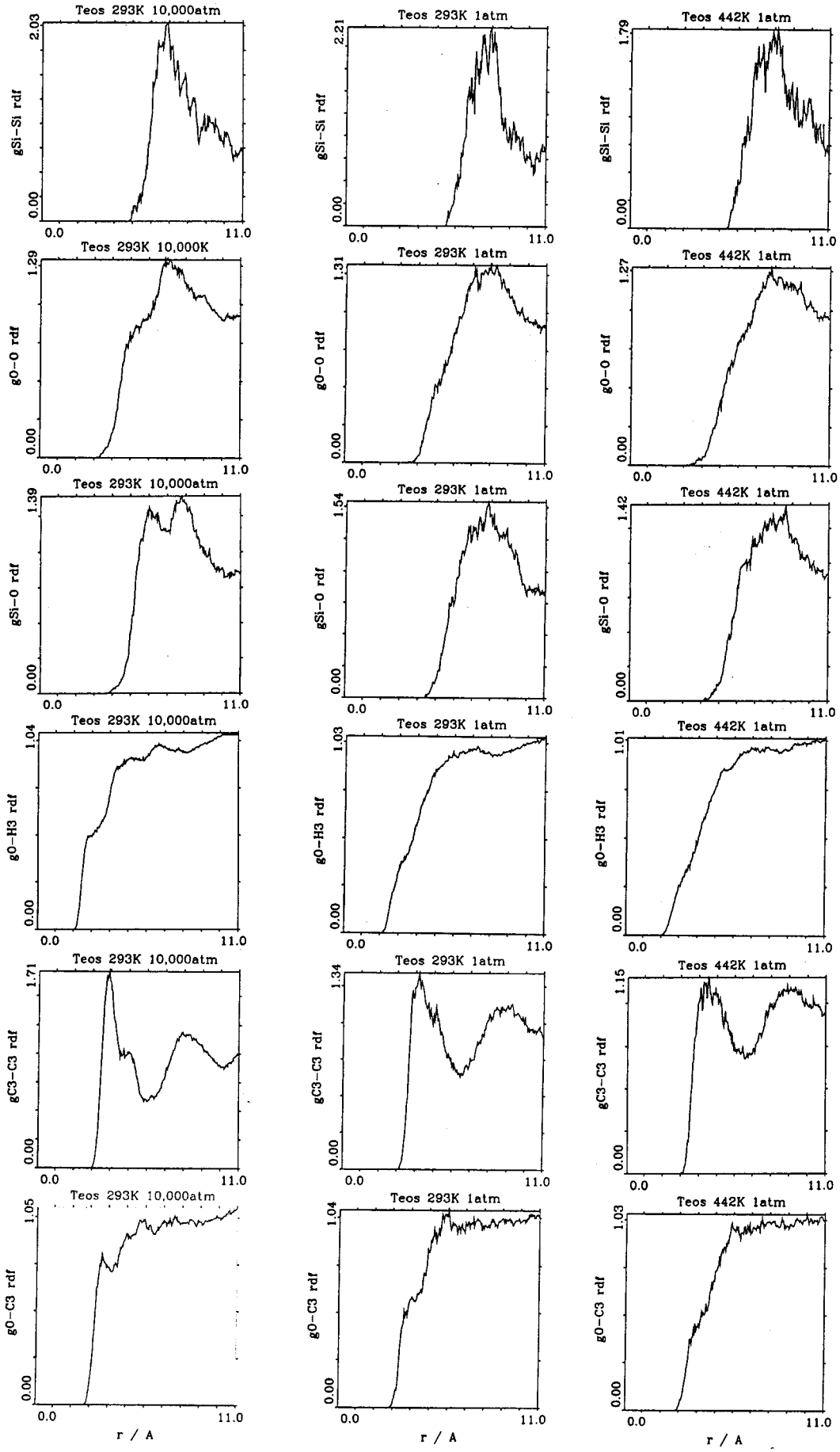

Figure 7. Intermolecular pair-distribution functions in TEOS for a pressure of 10 000 or 1 atm and a temperature of 20 or 169 °C, from atom-based (DL_POLY) simulations with an Ewald sum, after 24.0 ps of equilibration time and 1.0 ps of collecting time.

second peak, at about 4.8 Å in methanol, and at 5.2 Å in ethanol. At high pressure, the second peaks are shifted to smaller distances, an effect that is particularly visible in ethanol. In fact, temperature and pressure variations may cause greater changes in the structures of liquids with larger molecules. For both alcohols, a third peak can be seen at about 7.0 Å, at high pressure.

The O−H (O−D) interactions in water, heavy water, methanol, and ethanol show two important peaks, the first between 1.9 and 2.0 Å and the second at about 3.5 Å. However, in water and heavy water the second peak is more important, whereas in the alcohols this peak is relatively small and the first peak is predominant. This first peak represents the hydrogen bonds, which in water, in the gas phase, occur at ≈1.98 Å, as shown in refs 40 and 31. Although these distributions are in agreement with Jorgensen's results,[8] it is unclear why the hydrogen-bond peak is so weak in water. A third peak appears in water and heavy water at about 6.0 Å; it is visible in methanol at 5.0 Å and cannot be seen in ethanol.

Because the H−H interactions are, in general, much weaker (because of the smaller charges and van der Waals repulsion and dispersion), the corresponding RDFs could be expected to show much less structure. This is the case in water and heavy water, but definitely not in the alcohols. In water and heavy water, there are very small peaks, at 2.5 and 4.0 Å, the second one becoming just a shoulder, at high pressure. In the alcohols, the first peak appears at 2.5 Å, but is very pronounced; and the second peak, even at high pressure, appears only at 5.0 Å. These features are also in agreement with Jorgensen's results.

These interactions between hydroxyl groups may be compared with interactions between alkyl groups in methanol and ethanol. The C−C interaction in methanol shows a pronounced peak at about 4.2 Å and a well-defined second peak at about 8.0 Å, so there are significant structural features concerning the more apolar alkyl groups. The C_3-C_3, C_3-C_2, and C_2-C_2 interactions in ethanol are all very similar at ambient conditions and are fairly close to the corresponding C−C interaction in methanol, although the first peak is less defined and the second is displaced to 9.0 Å. The relatively broad C_3-C_3 first peak in ethanol splits at high pressure into two perfectly separated peaks, at 4.0 and 5.0 Å, an effect which is not observed in methanol. Additionally, the structure of the C_2-C_2 interaction in ethanol becomes poorly defined at high temperature.

These C−C interactions in methanol and ethanol are very similar to the equivalent C−C and C_3-C_3 interactions in TMOS and TEOS. In both cases, the first peak appears at 4.2 Å but is smaller in the alkoxides. The second peak occurs at about 8.0 Å in TMOS and at about 9.0 Å in TEOS, as in methanol and ethanol, respectively. As can be seen by the peak and shoulder appearing at high pressure, the first C_3-C_3 peak in TEOS in fact comprises two peaks, one at about 3.9 Å and a second at about 4.0 Å, as in the same interaction in ethanol. The CH_3-CH_3 interactions are thus almost equal in $Si(OCH_3)_4$ and CH_3OH, and in $Si(OCH_2CH_3)_4$ and CH_3CH_2OH, but are slightly different between $Si(OCH_3)_4$ and $Si(OCH_2CH_3)_4$ or between CH_3OH and CH_3CH_2OH, showing that these interactions depend more on the alkyl groups involved than on the other chemical characteristics of the molecules.

The interactions between hydroxyl and alkyl groups can be analyzed by looking at the C−O and $C-H_o$ interactions in methanol and the C_2-O, C_3-O, C_2-H_o, and C_3-H_o, interactions in ethanol. In all three C−O interactions, the first peak occurs at about 3.5 Å, but the second, at about 5.0 Å, is very weak in methanol and is displaced to 6.0 Å in ethanol in the C_2-O interaction. At 10 000 atm, these three interactions become very similar and even a broad third peak can be seen, at 7.5 Å in methanol and 8.0 Å in ethanol.

The $C-H_o$ and C_2-H_o interactions in methanol and ethanol are very similar, particularly at high pressure. They show four well-defined peaks, all systematically displaced to shorter distances in methanol, by about 0.5 Å compared with ethanol. Surprisingly, the C_3-H_o ethanol interaction is considerably different, showing only the second and third peaks and an incipient fourth one. The second peak is much more important than in the other two interactions, and the first peak definitely is not present. In both $C-H_o$ and C_2-H_o interactions, the carbon atom is bonded to a hydroxyl oxygen, which might attract more closely the H_o hydrogen, because of its higher charge. This would split the strong first peak observed in the C_3-H_o interaction into two much smaller ones, the first occurring at only 2.5−2.8 Å.

The O−C, O−H, and $O-C_3$, $O-H_3$ interactions in TMOS and TEOS should be very different from the O−C, O−H interactions discussed so far for water, methanol, and ethanol, because the oxygen atom is in a metalorganic group rather than a hydroxyl group. As expected, in both alkoxides, the O−H interactions start at shorter distances of about 2.2 Å compared with the O−C interaction, which starts, at 2.8 Å. The almost complete absence of structure, until the cutoff distance of 11.0 Å, for all four interactions shows that, probably because of steric hindrance, the interaction of the inner oxygen atoms with the outer alkyl groups is unimportant, even at high pressure.

The O−O interactions in both alkoxides show two peaks, the first of which is visible only in TEOS at high pressure. They occur at large distances of 4.5 and 5.5 Å in TMOS and TEOS, respectively. The Si−O RDFs for both alkoxides also show two distinct peaks, at 6.0−6.5 Å, which again, in the case of TEOS, are visible only at high pressure.

The first peak in the Si−Si pair function in TEOS occurs at about 7.5 Å, in good agreement with the distance of slightly over 7 Å reported by Yoldas for the Si−Si interaction in pure TEOS,[41] although the signal/noise ratio is not particularly good for the Si−Si RDFs calculated here, because of the small number (only 51) of Si atoms in these simulations. In TMOS, the corresponding first peak occurs at a slightly smaller distance of about 6.5 Å, but no experimental data is available with which to compare this result. In general, in all radial distribution functions discussed here, the compression and expansion effects due to the high pressure and temperature can clearly be seen.

Diffusion. We now move to the dynamic properties of the liquids by calculating the mean square displacement (defined as $\mathrm{MSD} = \langle|\vec{r}_i(t) - \vec{r}_i(0)|^2\rangle$) as a function of time for each atomic species in the liquid. In this work, we measured the MSDs for all liquids and thermodynamic conditions simulated, using both DISCOVER and DL_POLY. However, because the MSD is very sensitive to the state of equilibration of the system, large simulation times are required to get very accurate results. Figure 8 shows the total and partial *x*, *y*, and *z* mean square displacements measured for the oxygen atoms in water, methanol and ethanol, as a function of time, for 1 atm and 20 °C, after 50 ps (100 000 time steps) of sampling time. Equivalent simulations at high pressure or high temperature were not tried, because of the large CPU times involved.

The increase of the MSD with time is linear in water, methanol, and ethanol, showing that these systems are properly equilibrated. Moreover, for all liquids, the partial *x*, *y*, and *z* MSDs are essentially the same, as should be the case given that no overall translational motion is occurring during the liquid

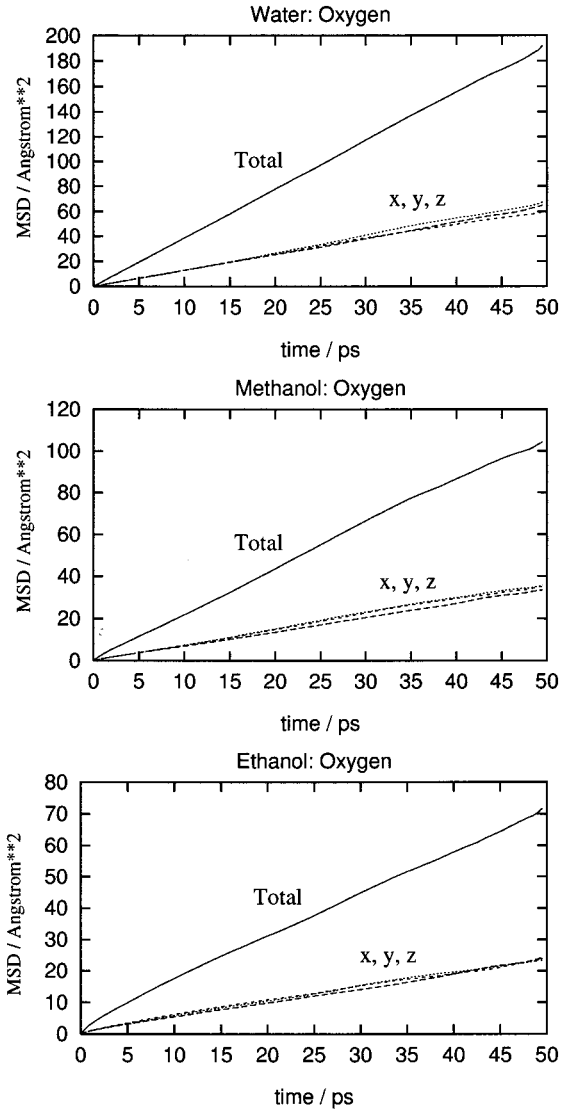

Figure 8. Mean square displacement (Å^2) as a function of time (ps) in water, methanol, and ethanol, at 1 atm and 20 °C, after 25.0 ps of equilibration and 50.0 ps of sampling time, from atom-based (DL_POLY) simulations with an Ewald sum.

simulation. These results compare very favorably with the MSD evolution noted in the shorter simulations, although there is still some oscillation, particularly for ethanol and the alkoxides.

In the shorter simulations (less accurate but available for a wider range of systems and conditions), we found that the MSDs in heavy water are almost as small as in methanol, whereas the values obtained for TMOS and TEOS are very similar, despite the different alkyl groups. As expected, the MSD evolution at high temperatures (boiling point) is better than at ambient condition, because the system is better equilibrated. At high pressures (10 000 atm), even increasing the sampling time from 2000 to 5000 time steps (2.5 ps), the results are unsatisfactory. However, no significant differences are observed between the partial MSDs, even in the alkoxides.

Because the average medium- and long-range interactions affecting a molecule are isotropic, increasing the pressure reduces residual differences between the partial MSDs, whereas on increasing the temperature, these differences tend to increase and kinetic translation motion becomes more probable. Clearly, both temperature and pressure affect very much the molecular displacement in liquids, and the effect increases with the size of the molecules.

The liquid self-diffusion coefficients, available experimentally from a large number of techniques,[42] can be calculated from the time evolution of the MSD, according to the Einstein equation:[33] $2tD = {}^1/_3$ (MSD). The self-diffusion coefficients for water, methanol, and ethanol, at ambient conditions, obtained from the long simulations, are shown in Table 10 and compared with experimental data. Self-diffusion coefficients for water, heavy water, methanol, ethanol, TMOS, and TEOS, at ambient conditions, high pressure and high temperature, obtained from the shorter simulations with both DL_POLY and DISCOVER, are also reported.

In general, for all cases considered, the calculated values are higher than the experimental results. The more accurate theoretical values, obtained with DL_POLY after 50 ps of sampling time, agree reasonably well with experiment for methanol (3.51×10^{-5} cm^2 s^{-1} compared with 2.10×10^{-5} cm^2 s^{-1}) and ethanol (2.41×10^{-5} cm^2 s^{-1} compared with 0.95×10^{-5} cm^2 s^{-1}), but are higher than expected for water (6.47×10^{-5} cm^2 s^{-1} compared with 2.15×10^{-5} cm^2 s^{-1}). For the shorter simulations using DL_POLY (sampling time = 1 ps), the agreement with the experimental results becomes poorer, as expected. The values calculated with DISCOVER are, in turn, considerably worse than the results obtained with DL_POLY, probably because of the less accurate simulation method used (group-based criteria, no Ewald sum, shorter time step and cutoff).

Self-diffusion coefficients are difficult to simulate because they are very sensitive to the modeling conditions, particularly temperature, force field, time step, equilibration time, and the NPT algorithm, as our results show. However, in the last two decades, better simulated values for the diffusion coefficients of water have been obtained. In particular, the Berendsen SPC model, with atomic charges that are very similar to the ones applied here, is reported to give good results for the self-diffusion coefficient of water at ambient conditions.[18]

The differences between the results obtained with the two models are most likely due to the effects of the intramolecular potentials, the NPT algorithm and the small temperature relaxation time. Intramolecular potentials aiming to simulate the atomic vibrational motions, such as the ones used here, should increase the atomic movements and therefore the diffusion coefficients. The NPT ensemble algorithm clearly has an important influence on the dynamical trajectories. The Berendsen algorithm used throughout this work is reliable, but it does not simulate well the thermodynamic fluctuations of an isothermic−isobaric system. Less constrained simulations, with larger Berendsen relaxation times or more sophisticated NPT algorithms (Parrinello-Rahman[43] or Nose-Hoover[44,45]), although they produce larger pressure and temperature fluctuations, may affect less the atomic force fields and the atomic trajectories, thereby decreasing the diffusion coefficients.

Another reason for the high diffusion coefficients calculated for water could be a deficient description of its hydrogen bonds, which decrease the mobility in the liquid and explain why the diffusion coefficients in water and methanol are almost equal (2.15×10^{-5} cm^2 s^{-1} compared with 2.10×10^{-5} cm^2 s^{-1}), despite the different number of atoms in each molecule. This argument is supported by the shift in the position of the second peak of the O−O radial distribution function in water, generally regarded as critical in describing the water medium-range structure, as discussed in the Radial Distribution Function section.

Given the importance of the dynamical aspects of these simulations in our future work, we plan to undertake a

TABLE 10: Calculated and Experimental Self-Diffusion Coefficients of Water, Methanol, Ethanol, TMOS, TEOS, and Heavy Water for Several Pressures and Temperatures, Obtained from DL_POLY (POLY) and DISCOVER (DISC) Simulations[a,b]

	Self-Diffusion Coefficient/10^{-5} cm^2 s^{-1}					
	H_2O	MeOH	EtOH	$Si(OMe)_4$	$Si(OEt)_4$	D_2O
			20 °C/10^4 atm			
POLY (24 + 1 ps)	3.55	1.52	0.91	0.23	0.26	
DISC (19.5 + 0.5 ps)	6.17	5.12	4.08	4.02		
Experimental	0.50					
			20 °C/1 atm			
POLY (25 + 50 ps)	6.47	3.51	2.41			
POLY (24 + 1 ps)	6.55	5.27	4.35	1.73	1.58	5.43
DISC (19.5 + 0.5 ps)	7.67	9.03	8.14	5.54		
Experimental	2.15	2.10	0.95			
			T_b/1 atm			
(T_b/°C)	(100.0)	(64.5)	(78.3)	(121)	(169)	
POLY (24 + 1 ps)	11.05	7.23	8.47	3.57	4.47	
Experimental	6.60		3.00			
			80°C/1 bar			
DISC (19.5 + 0.5 ps)	11.29	11.93	12.40	7.20		
Experimental	6.20		3.00			

[a] Experimental values from ref 42. [b] Values for MeOH and EtOH at 80 °C are extrapolations.

systematic study of the influence of all these variables on the diffusion coefficients. The fact that the same trends are observed for all liquids and conditions studied is encouraging. Correcting the self-diffusion coefficient in, say, water in ambient conditions may lead to good dynamic properties for all liquids and thermodynamic conditions. Of course, reliable and accurate self-diffusion coefficients rely on the rigorous calculation of the mean square displacements or velocity autocorrelation functions, which is still a difficult task for liquids with large molecules such as the alkoxides.

4. Conclusions

The results reported here show that it is possible to simulate different liquids and thermodynamic conditions with molecular dynamics, using both the same general methodology and same types of interatomic potentials.

The DL_POLY results obtained with an atom-based criterion and an Ewald sum confirm and extend the DISCOVER results previously calculated with a group-based criterion and a Coulombic cutoff. The densities and enthalpies of vaporization calculated with DL_POLY are slightly more accurate than before. Despite its larger size, TEOS can now be simulated for any conditions of pressure and temperature, because of the atom-based criterion applied with DL_POLY. Liquid heavy water was also studied with DL_POLY, as it might provide a way to investigate in the future isotopic effects in liquid solutions. The radial distribution functions are essentially the same as with DISCOVER and agree well with experimental data. However, the self-diffusion coefficients are still slightly higher than the experimental values. In the future it is important to study in more detail the dynamics of these systems, particularly for NVE and NPT ensembles.

The similarity of the results obtained with DISCOVER and DL_POLY, which have slightly different implementations and force fields, for a whole range of liquids and thermodynamic conditions show the basic strength and correctness of the potentials and general methodology adopted in these studies. It is very encouraging that such a range of different liquids, thermodynamic conditions, and properties, can be simulated with reasonable accuracy, using throughout the same potentials and procedures. In the future, the methodologies used here should allow us to prepare automatically solutions formed by the mixture of simple liquids, without requiring systematic and expensive analysis—a key result to assist further studies of complex liquid solutions by molecular dynamics and other molecular simulation methods.

Acknowledgment. We are grateful to EPSRC for funding the local and national computer facilities used for this work. We are grateful to MSI for providing the DISCOVER code and other software. J.C.G.P. is greatly indebted to JNICT, Programa Ciência and programa Praxis XXI, Lisboa, for their financial support.

Appendix A

Force Field. Five different sets of potentials are used for oxygen atoms: o, used in hydroxyl groups in methanol and ethanol; ohh, used only in water; oss, used in bridging oxygens in silicates; osh, used in terminal oxygens in silicates; and osc, used to simulate the metal−oxygen−carbon metalorganic bond in alkoxides. Bond lengths and bond angles in osc were obtained from our previous ab initio optimizations,[31,32] and the corresponding force constants were obtained directly or after geometric averages of other values (the force constant in Si−O and O−C was made equal to previous si−o and o−c interactions, whereas the force constant in Si−O−C was obtained from the geometric average of Si−O−Si and C−O−C force constants).

Three different sets of potentials are used for hydrogen atoms: ho, used in water and hydroxyl groups in alcohols; h2 or h3, used in methylene and methyl groups; and hos, used in hydroxyl groups in silicates. h2 and h3 are exactly the same; the different names are used only to facilitate the analysis of the results.

One set of potentials is used to simulate all carbon atoms: c2 (in the methylene groups) and c3 (in methyl groups). One set of potentials is used to simulate all silicon atoms: sz0, sz1, sz2, sz3, and sz4 (where the number represents the number of bridging oxygens, as in the NMR notation). In both cases, different names are given only to facilitate the analysis of the results.

Appendix B

Partial Charges. The magnitudes of the partial charges are fundamental to an adequate simulation of the intermolecular

TABLE 11: 2.7*Hirshfeld Partial Charges Used throughout this Work, in Atom-Based (DL_POLY) Simulations with an Ewald Sum, of Simple Liquids

	2.7*Hirshfeld Partial Charges	
H_2O	ohh: −0.8170	ho: 0.4085
CH_3OH	c3: −0.1820	h3: 0.1183
	o: −0.5943	ho: 0.4214
CH_3CH_2OH	c3: −0.3660	h3: 0.1323
	c2: −0.0626	h2: 0.0956
	o: −0.5783	ho: 0.4188
$Si(OCH_3)_4$	sz4: 1.2540	osc: −0.5535
	c3: −0.1479	h3: 0.1293
$Si(OCH_2CH_3)_4$	sz4: 1.2452	osc: −0.5416
	c3: −0.3610	h3: 0.1342
	c2: −0.0311	h2: 0.1099
$Si(OH)_4$	osh: −0.7673	hos: 0.4655
	sz0: 1.2072	
$Si_2O(OH)_6$	osh: −0.7266	hos: 0.4377
	sz1: 1.2415	oss: −0.7496

interactions in condensed matter. The partial charges used in all Ewald-based DL_POLY simulations are presented in Table 11. These were obtained by multiplying the Hirshfeld charges resulting from ab initio DMOL optimizations[31,32] of each single molecule by 2.7. Hirshfeld charges were used because they present the right trends, from the chemical point of view. To fit the experimental densities and enthalpies of vaporization, the multiplicative factor applied in these calculations is slightly larger than in the previous DISCOVER cutoff-based MD calculations, 2.6. The charges presented here are very similar to cvff and cff91 charges proposed in reference 28 and to charges previously reported by Jorgensen[9] and Berendsen.[18]

Appendix C

Dipoles versus Partial Charges. A simple way to check the physical plausibility of a proposed set of partial charges is to calculate the corresponding electric dipole moment for each of the molecular aggregates and compare the result with experiment. Table 12 shows the electrical dipole moment for each kind of molecule occurring in the liquids studied here.

TABLE 12: Experimental and Calculated Dipole Moments of a Single Molecule of Water, Methanol, Ethanol, TMOS, and TEOS, with Hirshfeld Partial Charges, Multiplied by a Scaling Factor: 2.7[a]

	Dipole/Debye	
mol	cal	exp
water	1.85_{gas}[46]	
	2.28	$2.01-3.00_{liq}$[46]
ethanol		
(trans−gauche)	1.68−2.30	$1.44-1.68_{gas}$[47]
methanol	2.13	1.70_{gas}[47]
TEOS	0.001−1.67	1.63_{liq}[36]
TMOS	0.000	1.171_{liq}[36]

[a] Experimental values from refs 36, 46, and 47.

The calculated values were obtained after a long period of equilibration (typically 100 ps), followed by a static energy minimization. The electric dipole moment for ethanol was calculated for both trans and gauche conformations. It can be seen that these scaled Hirshfeld charges, obtained from the full optimization of each isolated cluster, reproduce the experimental densities without leading to unrealistic values for μ_{cal}.

In the liquid phase, the electrostatic induction of atoms on each other tends to increase the electric dipole moment, as can be seen for water. This enhancement effect is correctly described

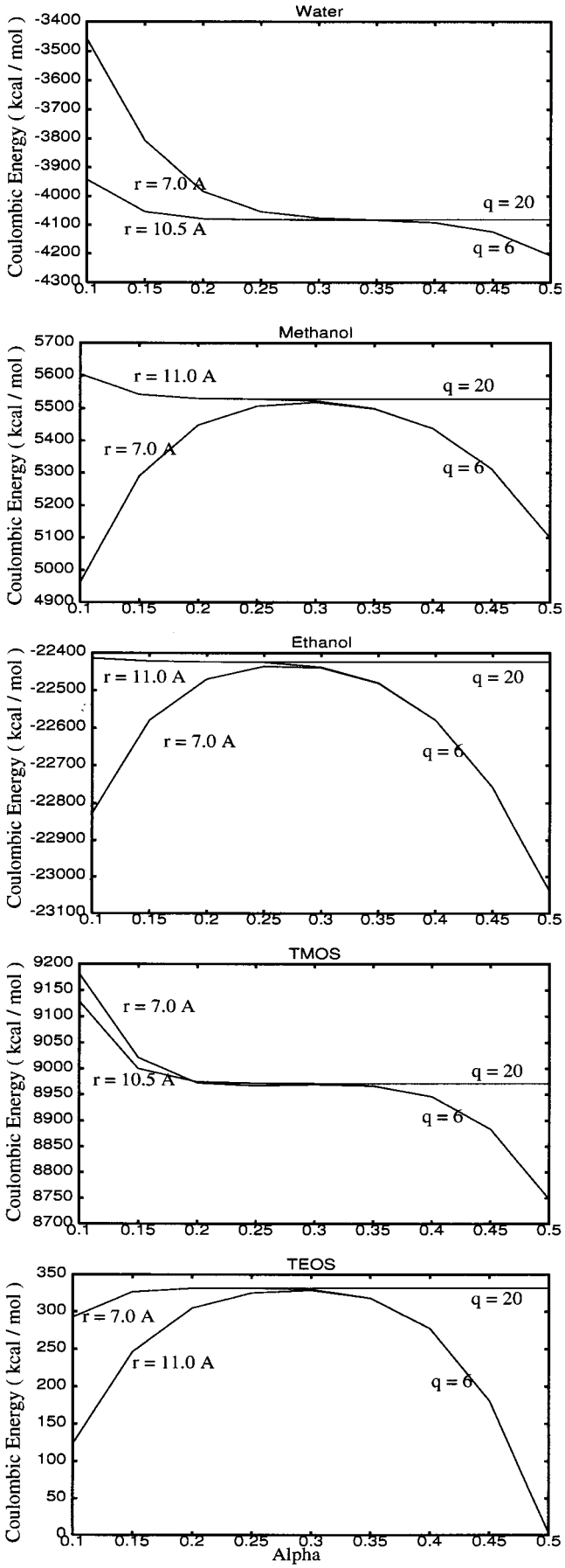

Figure 9. Coulombic energy at ambient conditions as a function of the Ewald sum parameter α, for a real-space cutoff of 7.0 or 10.5 Å (water, TMOS)−11.0 Å (methanol, ethanol, TEOS) and a reciprocal-space cutoff of 6 or 20 vectors.

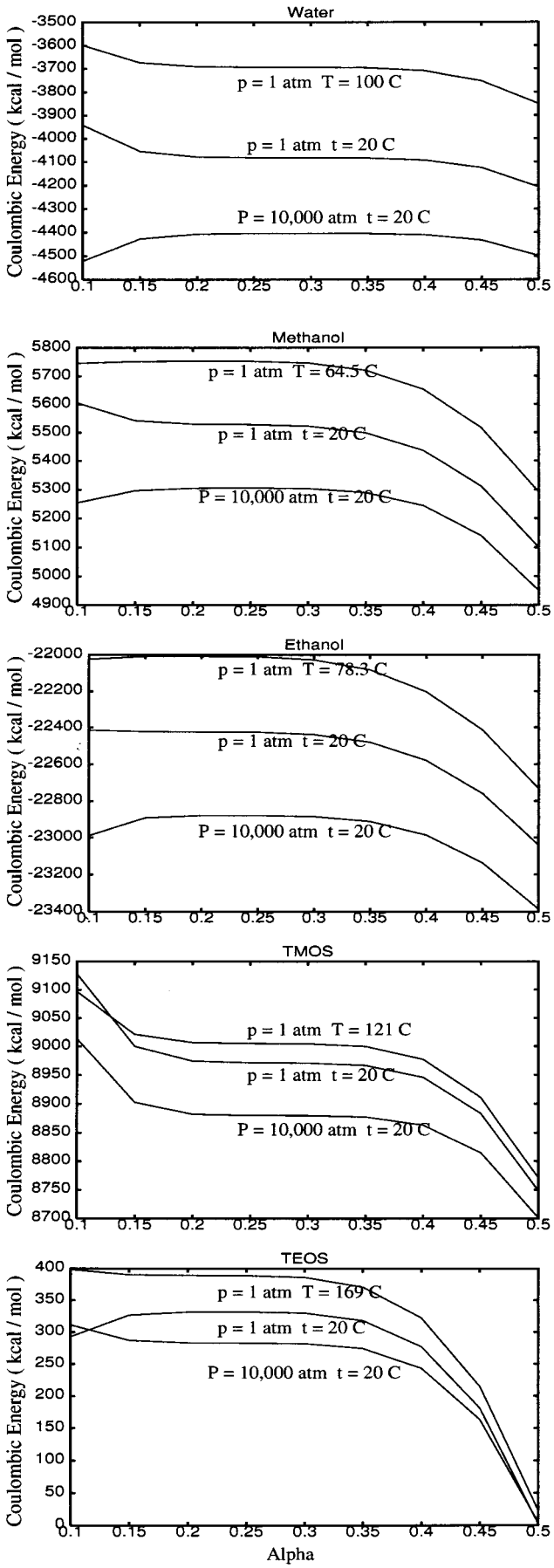

Figure 10. Coulombic energy at several different conditions of pressure and temperature as a function of the Ewald sum parameter α, for r_{max} = 10.5 A (water, TMOS)−11.0 Å (methanol, ethanol, TEOS) and q_{max} = 6.

by the various sets of charges proposed to simulate liquid water, methanol, and ethanol. Although the electric dipole of TEOS and TMOS should be very small in the gas state, because of symmetry considerations, as is corroborated by our values, it is reported to be quite high in the liquid state, because of important polarizability effects.

Appendix D

Ewald Sum. The Coulombic energy of water, methanol, ethanol, TMOS, and TEOS, as a function of the Ewald sum parameter α, is presented in Figure 9, at ambient conditions. Clearly, a flat plateau is observed for all these systems, where the Coulombic energy does not change with the value of the parameter α. In this region, the Ewald sum achieves convergence for small real- and reciprocal-space cutoffs, as it does not change with small modifications in α, r_{max} or q_{max}. This finding is important, as the calculation of the Ewald sum is usually one of the most time-consuming steps in MD simulations.

Furthermore, this plateau occurs in exactly the same region for all systems. This means that the same α, r_{max} and q_{max} parameters can be used for systems with different composition, including even chemical reactions, where the composition necessarily changes with time.

The variation of the Coulombic energy with the α parameter is presented in Figure 10 for the same liquid systems, for ambient conditions, very high pressure, and very high temperature. Although the Coulombic energy is obviously different for different thermodynamic conditions, becoming more negative with the degree of condensation of the system, the flat region occurs always in the same range of α; this shows that totally different conditions of pressure and temperature can be studied using the same Ewald sum parameters, for example, in the simulation of chemical reactions.

References and Notes

(1) Barker, J. A.; Watts, R. O. *Chem. Phys. Lett.* **1969**, *3* (3), 144.
(2) Rowlinson, J. S. *Liquids and Liquid Mixtures*; Butterworth: London, 2nd ed.; 1969.
(3) Rahman, A.; Stillinger, F. *J. Chem. Phys.* **1971**, *55* (7), 3336.
(4) Narten, A. H.; Levy, H. A. *J. Chem. Phys.* **1971**, *55* (5), 2263.
(5) Stillinger, F. H. *J. Chem. Phys.* **1974**, *60* (4), 1545.
(6) Stillinger, F. H. *Adv. Chem. Phys.* **1975**, *31*, 1.
(7) McDonald, I. R.; Klein, M. L. *J. Chem. Phys.* **1978**, *68* (11), 4875.
(8) Jorgensen, W. L. *J. Am. Chem. Soc.* **1981**, *103*, 335.
(9) Jorgensen, W. L. *J. Chem. Phys.* **1982**, *77* (7), 4156.
(10) Jorgensen, W. L. *J. Am. Chem. Soc.* **1981**, *103*, 341.
(11) Jorgensen, W. L. *J. Am. Chem. Soc.* **1981**, *103*, 345.
(12) Jorgensen, W. L.; Ibrahim, M. *J. Am. Chem. Soc.* **1981**, *103*, 3976.
(13) Jorgensen, W. L.; Binning, R. C.; Bigot, B. *J. Am. Chem. Soc.* **1981**, *103*, 4393.
(14) Jorgensen, W. L. *J. Am. Chem. Soc.* **1981**, *103*, 4721.
(15) Andrea, T. A.; Swope, W. C.; Andersen, H. C. *J. Chem. Phys.* **1983**, *79* (9), 4576.
(16) Stillinger, F. H.; Rahman, A. *J. Chem. Phys.* **1978**, *68* (2), 666.
(17) Jorgensen, W. L.; Chanrasekhar, J.; Madura, J. D. *J. Chem. Phys.* **1983**, *79* (2), 926.
(18) Berendsen, H. J. C.; Grigera, J. R.; Staatsma, T. P. *J. Phys. Chem.* **1987**, *91*, 6269.
(19) Fincham, D. *Mol. Simul.* **1994**, *13*, 1.
(20) Kolafa, J.; Perram, J. W. *Mol. Simul.* **1992**, *9* (5), 351.
(21) Rycerz, Z. A.; Jacobs, P. W. M. *Mol. Simul.* **1992**, *8*, 197.
(22) Rycerz, Z. A. *Mol. Simul.* **1992**, *9* (5), 327.
(23) Strauch, H. J.; Cummings, P. T. *Mol. Simul.* **1989**, *2*, 89.
(24) Honda, K.; Kitaura, K.; Nishimoto, K. *Mol. Simul.* **1991**, *6* (4), 275.
(25) Casulleras, J.; Guardia, E. *Mol. Simul.* **1992**, *8*, 273.
(26) Kumagai, N.; Kawamura, K.; Yokokawa, T. *Mol. Simul.* **1994**, *12* (3), 177.
(27) Brodholt, J.; Wood, B. *J.f Geophys. Res.* **1993**, *98*, 519.
(28) *Discover 96.0 manual*; Molecular Simulations Inc.: San Diego, CA, 1996.

(29) DL_POLY *manual*; S.E.R.C. Daresbury Laboratory: Cheshire, U.K., 1996.
(30) Hill, J.; Sauer, J. *J. Phys. Chem.* **1994**, *98*, 1238.
(31) Pereira, J. C. G.; Catlow, C. R. A.; Price, G. D. *J. Phys. Chem.* **1999**, *103*, 3252.
(32) Pereira, J. C. G.; Catlow, C. R. A.; Price, G. D. *J. Phys. Chem.* **1999**, *103*, 3268.
(33) Allen, M. P.; Tildesley, D. J. *Computer Simulation of Liquids*; Oxford Science Publications: Oxford, U.K., 1987.
(34) *International Critical Tables*, 1st ed.; McGraw-Hill: New York, 1928; Vols. III and V.
(35) Dean, J. A. *Lange's Handbook of Chemistry*, 14th ed.; McGraw-Hill: New York, 1992.
(36) Brinker, C. J.; Scherer, G. W. *The Physics and Chemistry of Sol−Gel Processing*; Academic Press Inc.: New York, 1989.
(37) Perry, R. H. *Chemical Engineers Handbook*, 5th ed.; McGraw-Hill: New York, 1969.
(38) *Handbook of Chemistry and Physics*; CRC Press: Cleveland, OH, 1994.
(39) *Silicon, Germanium, Tin amd Lead Compounds, Metal Alkoxides, Diketonates and Carboxylates: A Survey of Properties and Chemistry*; ABCR GmbH + Co.: Karlsruhe, 1995.
(40) Umeyama, H.; Morokuma, K. *J. Am. Chem. Soc.* **1977**, *99* (5), 1316.
(41) Yoldas, B. E. *J. Non-Cryst. Solids* **1986**, *82*, 11.
(42) Johnson, P. A.; Babb, A. L. *Chem. Rev.* **1956**, *56*, 387.
(43) Parrinello, M.; Rahman, A. *J. Appl. Phys.* **1981**, *52* (12), 7182.
(44) Nose, S. *J. Chem. Phys.* **1984**, *81* (1), 511.
(45) Melchionna, S.; Ciccotti, G.; Holian, B. L. *Mol. Phys.* **1993**, *78* (3), 533.
(46) *Tables of Physical and Chemical Constants*, 14th ed.; Kaye, G. W. C., Laby, T. H., Eds.; Longman: London, New York, 1973.
(47) James, A. R. *Macmillan's Chemical and Physical Data*; Macmillan Press Ltd.: London, 1992.